Ultrasonics 61 (2015) 103–113

Contents lists available at ScienceDirect

Ultrasonics

journal homepage: www.elsevier.com/locate/ultras

Prediction of ultrasonic pulse velocity for enhanced peat bricks using adaptive neuro-fuzzy methodology

Shervin Motamedi [a,b], Chandrabhushan Roy [a], Shahaboddin Shamshirband [c,*], Roslan Hashim [a,b,*], Dalibor Petković [d], Ki-Il Song [e]

[a] Department of Civil Engineering, Faculty of Engineering, University of Malaya, 50603 Kuala Lumpur, Malaysia
[b] Institute of Ocean and Earth Sciences, University of Malaya, 50603 Kuala Lumpur, Malaysia
[c] Department of Computer System and Information Technology, Faculty of Computer Science and Information Technology, University of Malaya, 50603 Kuala Lumpur, Malaysia
[d] University of Niš, Faculty of Mechanical Engineering, Department for Mechatronics and Control, Aleksandra Medvedeva 14, 18000 Niš, Serbia
[e] Department of Civil Engineering, Inha University, 100 Inha-ro, Nam-gu, Incheon 402-751, South Korea

ARTICLE INFO

Article history:
Received 9 November 2014
Received in revised form 3 March 2015
Accepted 6 April 2015
Available online 15 April 2015

Keywords:
Peat
Ground improvement
Ultrasonic pulse velocity
ANFIS
Estimation

ABSTRACT

Ultrasonic pulse velocity is affected by defects in material structure. This study applied soft computing techniques to predict the ultrasonic pulse velocity for various peats and cement content mixtures for several curing periods. First, this investigation constructed a process to simulate the ultrasonic pulse velocity with adaptive neuro-fuzzy inference system. Then, an ANFIS network with neurons was developed. The input and output layers consisted of four and one neurons, respectively. The four inputs were cement, peat, sand content (%) and curing period (days). The simulation results showed efficient performance of the proposed system. The ANFIS and experimental results were compared through the coefficient of determination and root-mean-square error. In conclusion, use of ANFIS network enhances prediction and generation of strength. The simulation results confirmed the effectiveness of the suggested strategies.

1. Introduction

Researchers have shown growing interest in non-destructive testing techniques to measure the compressive strength of construction materials because of their evident advantages. Some of these techniques are pulse-echo [1], impact-echo [2], ultrasonic pulse velocity [3], resonant frequency measurements [4], wave reflection methods [5], and acoustic emission methods [6]. This paper introduces a novel approach to estimate propagation of the ultrasonic pulse velocity (UPV) in construction materials, such as peat bricks, using the adaptive neuro-fuzzy methodology.

In recent decades, the energy consumption has multiplied due to fast industrialization. In line with this, construction industry requires alternative materials to replace the conventional compositions. Especially, brickworks seek alternative materials over the inefficient conventional compositions. For example, brick manufacturers consider the peat with relatively high organic content as a sustainable alternative for the traditional materials (i.e. aggregates). The use of peat decreases the density, and increases the brick's porosity and permeability, which in turn reduces the production expenditure. Nonetheless, the compressive strength of peat bricks as the key performance indicator, still highly relies on the content of the cementation agents [7,8].

The use of UPV has been widely investigated for the non-destructive estimation of concrete quality. Many empirical equations were introduced to evaluate the compressive strength of the cementitious materials based on the non-destructive testing variables [9–11]. The old method for mathematical relationship using compressive tests and the UPV on cementitious material samples through regression analysis was not effective [12,13]. A correlation between compressive strength and UPV of concrete was reported for some combinations [14]. The study simultaneously measured the pulse velocity and compressive strength of 150-mm cubes at different ages from 1 day to 28 days and revealed a linear relation between the strength and velocity. Lin et al. [15] carried out an experimental study to establish mathematical models for predicting concrete pulse velocity based on aggregate content and water–cement ratio. Sahu and Jain [16] used the UPV as measure of concrete quality for different structural components, such as roof beams, crane girders, shell beams, columns, and shell roof.

The UPV has been mainly reported to predict the compressive strength of cementitious materials through linear regression analysis using few parameters. Notwithstanding, adaptation of soft computing methodologies to estimate the physic-mechanical

* Corresponding authors at: Department of Civil Engineering, Faculty of Engineering, University of Malaya, 50603 Kuala Lumpur, Malaysia (R. Hashim), tel.: +60146266763 (S. Shamshirband).
E-mail addresses: shamshirband@um.edu.my (S. Shamshirband), roslan@um.edu.my (R. Hashim).

http://dx.doi.org/10.1016/j.ultras.2015.04.002
0041-624X/

properties as well as association between the UPV and compressive strength of peat-enhanced mixtures, especially the peat-bricks, have not been studied.

Application of artificial intelligence techniques is growing to examine structural components [17]. Although several mathematical functions are used to model the construction materials' UCS, disadvantages including extended calculation time should not be disregarded. The ANN's calculation power can be possibly used for the analytical methods. Some of the advantages of ANN are fast computation, independence from the information about internal system variables, and the compressed solution technique for multi-variable problems.

The current study aimed to accurately estimate UPV of peat bricks using ANFIS. To achieve that, a series of input and output parameters were obtained through laboratory experiments. The output parameter was the UPV of peat bricks, and input variables were percentage of peat, sand and cement content and curing period in days. The results of this study can be beneficial for future studies to determine the compressive strength of peat bricks using non-destructive testing methods.

2. Experimental methods

This study used a combination of experimental tests, soft computing technique (ANFIS), and sensitivity analysis to analyze peat–cement–sand based mixture.

2.1. Ultrasonic pulse velocity

The UPV has been employed to evaluate properties of cement-based materials through non-destructive technique [18]. A detailed description of UPV test can be found in the *Test for Pulse Velocity through Concrete* ASTM C 597-83 report [19].

The UPV test measures the speed of ultrasonic pulse through a concrete-based material. This value can be used to determine compressive strength of cementitious material. Correlations among compressive strength, the pulse velocity and elastic modulus were formerly reported [18,20,21]. Also, Whitehurst [22] stated relationship between pulse velocity and the concrete's compressive strength. Tharmaratnam and Tan [23] proposed an empirical equation showing relationship between unconfined compressive strength (UCS) and the concrete's UPV through the following function:

$$\mathrm{UCS} = a\, e^{bV} \tag{1}$$

where the properties of material determine a and b and V is the speed of ultrasonic pulse.

2.1.1. UPV experimental setup

In this study, the UPV test setup (in accordance with the ASTM C597-09 [19]) consisted of two transducers, data acquisition unit and a time measuring device, as shown in Fig. 1. This study measured the speed of ultrasonic wave (*P*-waves) using a pair of 50 kHz transducers. A 10 MHz pulse-receiver unit was used for exiting emitting transducer, and for conditioning the receiving transducer. Direct transmission was applied to the test specimen along 22 cm of the length. The test specimen was placed in contact with two transducers as shown in Fig. 1(a). A schematic circuit of pulse velocity test is shown in Fig. 1(b). At initial stage, the transducer-1 (transmitter) vibrates at the fundamental frequency, emitting the ultrasonic pulse. The vibrations travel through the test specimen and are received by the second transducer-2 (receiver) at the other end. The time measurement device indicates the time of ultra-sonic wave travel through the medium. The pulse velocity was determined as follows:

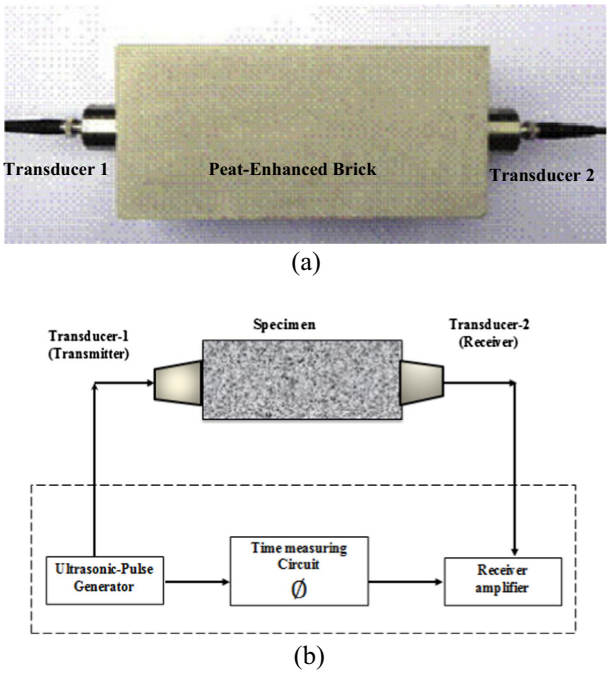

Fig. 1. (a) Setup of transducers and test specimen, (b) schematic diagram of pulse velocity testing circuit.

$$V = \frac{L}{t} \tag{2}$$

where L is the specimen length (peat–cement–sand brick with length of 22 cm), V is the pulse velocity (km/s) and t is the actual travel time through medium.

Investigators should ensure that the specimen has smooth surface at the point of contact with the transducers [24]. In addition, it is important that the surface is free of impurities, contamination or other heterogeneous particles. If impurities exit on the surface, they must be removed before the measurement.

2.1.2. Relationship between UPV and mechanical properties of cementitious materials

Density and elasticity of construction materials determine the velocity of ultrasonic pulses [25–27]. Thus, the velocity of ultrasonic pulse depends on the mechanical properties of the cementitious materials, such as cement type, mix proportions, type of aggregate, permeability, porosity, density, cement hydration, curing, water cement ratio, and manufacturing process [25,27–30]. The complexity in the inner structure of cementitious materials is governed by their constituents, such as (i) cement paste, (ii) mineral aggregates, and (iii) interfaces between aggregate particles and paste. This complexity leads to irregularity in ultrasonic waves, which interferes with non-destructive tests [26]. For example, the size of aggregate influences the ultrasonic pulse velocity. Probably, larger aggregates have higher pulse velocity, which depends on the mix design [29].

In addition to the mechanical properties, the production process also determines the behavior of UPV. For instance, increase in curing period amplifies the UPV values. Longer curing period increases the UPV due to alteration in the ratio of gel/space in longer curing period. This is because at the early stages of hydration, the air bubbles and the air/water phase in the cement paste in the water governing the UPV value [1,15,31,32]. On the other hand, increase of oxygen permeability and porosity decreases the UPV value. This indicates that the ultrasonic pulse travels faster through the solid than the void [17]. Recent efforts by Islam et al. [33] showed the

effect of peat presence on cement–sand–bricks. A connection was found between the UPV and the wet compressive strength of peat-enhanced bricks. Therefore, it was concluded that reduction in the compressive strength leads to drop of UPV values for cementation products.

2.2. Unconfined compression testing

Series of UCT were carried out along with the ASTM C 165 of bricks (the Standard Test Methods for Measuring Compressive strength). The test samples were weighed with an accuracy of 0.01 g before the UCT tests. Further, the test samples were openly pressed between double-coated plywood sheets (thickness of 3 mm). The testing machine had a capacity of 2500 kN and the rate of load application until failure was 3.5 N/mm^2/min. Sections 4.1.3–4.1.5 provide detailed discussion on the UCS results obtained from the UCT tests on the samples.

3. Experimental program

3.1. Preparation of samples

A total of 144 cuboid peat brick samples, each 22 cm in length, 5 cm in height and 10 cm in width, were compressed according to the ASTM D 698 (Standard Test Methods for Laboratory Compaction Characteristics of Soil Using Standard Effort) to ensure sufficient compaction and uniformity of porosity in samples. The samples were also tested in compliance with the ASTM D 2166. Fig. 2 shows the samples that were prepared before testing. The samples contained 0–30% peat and 20–30% cement (Table 1). The peat and cement contents varied in steps of 2% and 5%, respectively. The curing periods after 1, 7, 14, and 28 days were used to determine the mixture's strength. Three samples for each mix design were tested, and the results were averaged to avoid impact of any relevant errors. The densities of the samples were measured prior to testing. Table 1 presents the mix design for the samples series.

First, the peat soil was mixed with sand, and then it was further modified by addition of cement. The percentages of replacement between the peat and sand were taken as weight replacements. For example, 5% replacement of peat soil means that 5% of the corresponding sand weight was exchanged by the peat. As soon as the dry compounds were mixed properly, the water was added gradually until the optimum moisture content was reached. Then, the brick mold was fully filled with the fresh mixes. Without any delay, the mix was pressed into the mold.

The volume of brick was kept constant during the use of hydraulic jack machine. In order to control the pressure, the device was equipped with a load cell and data-logger. After 7–10 min of operation, the compaction pressure was applied to reach to 10 MN/m^2. In addition, the compaction effort was observed during the investigation for different soil mixes. The bricks were pressed along the longitudinal axis (220 mm in length).

After compaction the fresh 100 mm (width), the bricks were extruded from the press and cured for one day. Furthermore, the bricks were casted in concrete plinths and kept under polythene to persevere the initial moisture. After one day, the bricks were stacked on the top of each other and further cured under the polythene sheets in humid condition. All the bricks were tested for 1, 7, 14, and 28 days following pressing. The appearance of the peat bricks is shown in Fig. 2.

Fig. 2. Appearance of the peat bricks samples.

Table 1
Percentage of peat and cement in specimens.

Material	Percentage (%)
Peat	0, 2, 4, 6, 8, 10, 12, 14, 16, 18, 20, 22, 24, 26, 28, 30
Cement	20, 25, 30

3.2. Materials

3.2.1. Peat

The peat was used throughout this study. The peat mainly comprises of plant–rotten soil with high organic content of over 75% [34]. During the stabilization process, many factors affect stabilization of peat, including the high water content, low solid content, low pH values, and the environment. The physical and chemical components of peat change biologically and chemically over the time. The peat used in this study was collected from Selangor, Malaysia. Table 2 summarizes the physical properties of the collected test sample. The chemical composition of peat was assessed using the X-ray fluorescence according to the ASTM C 311 (*Standard Test Methods for Sampling and Testing peat for Use in Portland Cement Concrete*). The summary of the results are presented in Table 3. Fig. 3 depicts the physical appearance of the peaty.

3.2.2. Cement

Cement is a synthetic material that is produced with the Portland clinker and contains approximately 5% gypsum. Cement is used in bricks as an important source of silica and alumina to form the silicate and aluminate hydrates. It develops bonding agent, which increases the strength of matrices. It was ground to obtain a particle size of 1–100 lm and specified surface area of 300–550 m^2/kg [35].

Cements are categorized into five types (I–V). In practice, the Portland cement of type I or II is utilized in construction [36,37]. This study used the Type I Portland cement. Table 3 lists the

Table 2
Peat's physical properties in this study.

Properties	Value
Dry density (γd)	0.194 Mg/m^3
Bulk density (γb)	1.1 Mg/m^3
Specific gravity (Gs)	1.48
Classification/von post	H4
Void ratio (e)	7.5
Fiber content (%)	80%
Loss on ignition (%)	98.5%
pH	4.6
Plasticity index (%)	40.1%
Plastic limit (%)	125.1%
Linear shrinkage (%)	5.6%
Liquid limit (%)	165.2%

Table 3
Chemical composition of cement sand and peat in this study.

Component	Cement (%)	Sand (%)	Peat (%)
Silica (SiO_2)	21.60	70.30	3.1500
Alumina (Al_2O_3)	6.280	19.20	0.8500
Iron oxide (Fe_2O_3)	3.700	0.033	0.6900
Phosphorus pent oxide (P_2O_5)	0.090	0.731	0.0310
Magnesium oxide (MgO)	0.890	0.390	0.2300
Calcium oxide (CaO)	66.23	2.15	0.3000
Sulphur trioxide (SO_3)	0.020	0.160	0.5300
Sodium oxide (Na_2O)	–	–	0.0300
Potassium oxide (K_2O)	0.63	3.750	0.0110
Chlorine (Cl)	–	–	0.0710
Titanium dioxide (TiO_2)	0.220	0.045	0.0069
Carbon dioxide (CO_2)	–	–	93.000
Manganese(II) oxide (MnO)	0.080	2.125	–
Zinc oxide (ZnO)	0.010	0.041	0.003

chemical compounds of the cement from the XRF according to the ASTMC 311. The cement's physical characteristic are listed in Table 4.

3.2.3. Sand

It was imperative to identify the type of sand that was used in this study. Stevens introduced a classification method for soil based on the dry sieving [38]. In this study, the sand was categorized as poorly-graded sand (SP) according to the ASTM D 2487 (*Standard Practice for Classification of Soils for Engineering Purposes*) and the Stevens' method [38]. Fig. 4 illustrates the particle size distribution of the sand, and Table 5 summarizes its physical properties. In addition, Table 2 lists the chemical compounds of the sand in accordance with the ASTMC 311 based on the XRF. The sand deposit was obtained from Selangor, Malaysia. Fig. 5 depicts the sand's physical shape used in this work.

3.3. Simulation program using adaptive neuro-fuzzy inference system

3.3.1. Neuro-fuzzy computing

Soft computing is a novel approach for the construction of systems that are computationally intelligent and have human-like capability within a specific domain [39]. These systems are supposed to adapt in changing environments, learn to do better and explain their decision making process. It is usually more beneficial in real-world problem solving to employ several computing methods in a synergistic way rather than building a system, exclusively based on one technique [40]. The result of such synergistic use of computing techniques is construction of complementary hybrid intelligent systems. Neuro-fuzzy computing facilitates design and construction of such intelligent systems. Firstly, neural networks recognize patterns and adapt to cope with evolving environments; and secondly, fuzzy inference systems use human knowledge and

Fig. 3. Physical appearance of the peat in laboratory condition.

Table 4
Physical characteristics of the cement in this study.

Physical index	Cement
Odor	Odorless
Color	Grey
Specific gravity (Gs)	3.04
Water requirement (%)	100
Moisture content (%)	0.06
Strength index – 7 days (%)	99
Strength index – 28 days (%)	100
Loss in Ignition (LOI) (%)	1.69

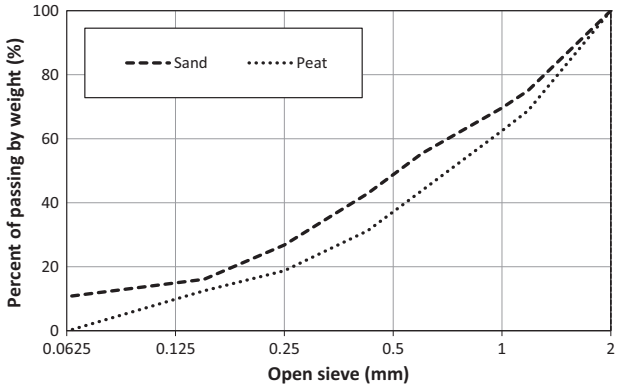

Fig. 4. Grading curve of peat and sand obtained through the particle size analysis.

Table 5
Physical characteristics of sand in this study.

Physical property name	Index properties
24-h water absorption (%)	25.12
Dry compacted bulk density (kg/m^3)	2.35
Specific gravity (Gs)	2.63
Dry bulk density (kg/m^3) Fineness	1928
Fineness modulus	2.84
Relative density	1.47

Fig. 5. Physical form of the sand at the laboratory condition.

implement decision making and differentiation [41]. The combination of these two complementary methodologies produces a novel discipline, called the neuro-fuzzy computing.

3.3.2. Adaptive neuro-fuzzy application

In this study, an ANFIS model was developed to predict the UPV based on a variation of input parameters (peat content, cement content, sand content and curing age). In order to train and check

the ANFIS network reliability, the UPV data was extracted according to the results of various compositions of cement, peat, sand in different curing periods.

The present study selected 3 bell-shaped functions of membership for every input variable with the maximum value of 1 and the least value of 0. The MATLAB Fuzzy logic toolbox was utilized consistently throughout the assessment and training processes of fuzzy interference system. The proposed ANFIS model in this study is illustrated in Fig. 6. As can be seen, there are four inputs including peat content, cement content, sand content and curing period.

In this study, the authors employed the first-order Sugeno model that included fuzzy IF–THEN rules developed by Takagi and Sugeno and two inputs [47–49],

if i is A and j is C and k is E and l is G then f_1

$$= p_1 i + q_1 j + r_1 k + s_1 k + t \tag{3}$$

The first layer involves the functions of input variables membership (MFs), which is merely responsible for supplying the values of input to the subsequent layer. Nodes of the first layer are adaptive nodes with node function, $O = \mu(i)$, where $\mu(i)_i$ are MFs.

Present study selected bell-shaped MFs with minimum equal to 0 and maximum equal to 1,

$$f(x; a, b, c) = \frac{1}{1 + \left(\frac{x-c}{a}\right)^{2b}} \tag{4}$$

where parameters a, b and c determine the bell-shaped function. Parameter b is mostly positive. As depicted in Fig. 7, parameter c is positioned at the middle of the curve.

The weight of each MFs is investigated in the second layer (membership layer). It accepts the input values from the 1st layer, and serves (as MFs) as fuzzy sets of the matching input variables. Nodes of the second layer are non-adaptive. This layer intensifies the received signals and transmits the following,

$$w_i = \mu(i)_i \cdot \mu(i)_{i+1} \tag{5}$$

Output of each node shows a rule or a weight's firing strength.

The 3rd (the rule) layer is non-adaptive in nature. Each neuron of the 3rd layer functions as the matching prerequisite of the fuzzy rules. That is, each rule's activation level is processed and the number of layers is equivalent to the quantity of fuzzy rules. Neuron of the third layer computes the normalized weights. Thus, each node evaluates the firing strength ratio of each rule as follows,

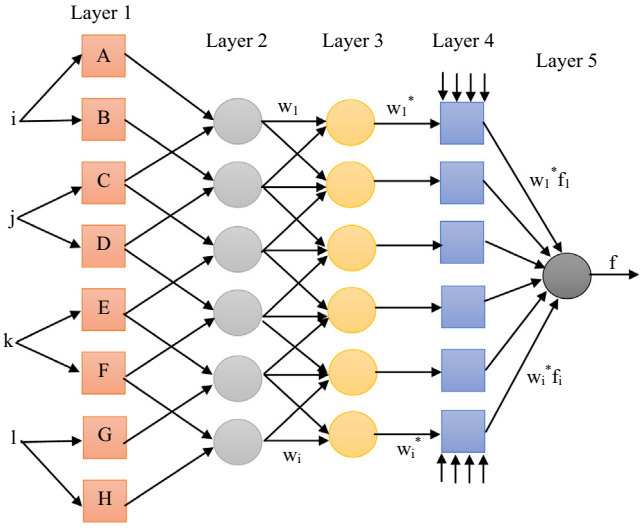

Fig. 6. Structure of the ANFIS model used in this study.

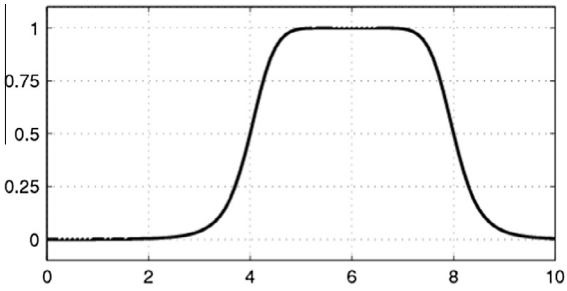

Fig. 7. Bell-shaped function of membership ($a = 2$, $b = 4$, and $c = 6$).

$$w_i^* = \frac{w_i}{w_1 + w_2} \quad i = 1, 2 \tag{6}$$

The outputs are termed as "normalized weights" or "normalized firing-strengths".

The fourth layer is called the defuzzification layer and provides the output values obtained from the rules' inference. In this layer, each node is adaptive with the function of:

$$O_i^4 = w_i^* \cdot f = w_i^* p_1 i + q_1 j + r_1 k + s_1 k + t \tag{7}$$

where $\{p_i, q_i, r_i, s_i, t\}$ is the parameter set. In addition, the parameters are consequent in this layer.

Finally, the 5th layer is known as the output layer. Within this layer, all input values are summed up from the previous layer (4th layer) and further transform the results of fuzzy categorization into crisp. It is noteworthy that a single node in the this layer is not adaptive. This node calculates final products as the total of all receiving signals,

$$O_i^5 = \sum_i w_i^* \cdot f = \frac{\sum_i w_i f}{\sum_i w_i} \tag{8}$$

3.3.3. Model performance evaluation

To evaluate the performance of measurement values and the ANFIS model, the statistical indicators were chosen as follows:

(1) Coefficient of determination (R^2)

$$\mathrm{RMSE} = \sqrt{\frac{\sum_{j=1}^{n} (O_i - P_i)^2}{n}}, \tag{9}$$

$$R^2 = \frac{\left[\sum_{i=1}^{n} (O_i - \overline{O_i}) \cdot (P_i - \overline{P_i})\right]^2}{\sum_{i=1}^{n} (O_i - \overline{O_i}) \cdot \sum_{i=1}^{n} (P_i - \overline{P_i})} \tag{10}$$

where P_i = measurement values, O_i = ANFIS value, and n = the total number of test data.

(2) Root-mean-square error (RMSE).

4. Results and discussions

This section discusses on the findings of the experimental study and ANFIS analysis.

4.1. Experimental results

4.1.1. Effect of peat-content on UPV

Fig. 8 illustrations changes in the UPV value by the peat content. In this study, samples with 20%, 25% and 30% cement contents were prepared. The graph shows UPV value for the samples with 25% cement, and increasing peat content from 0% to 30% with an interval of 2%. As can be seen, the UPV decreases with increase in

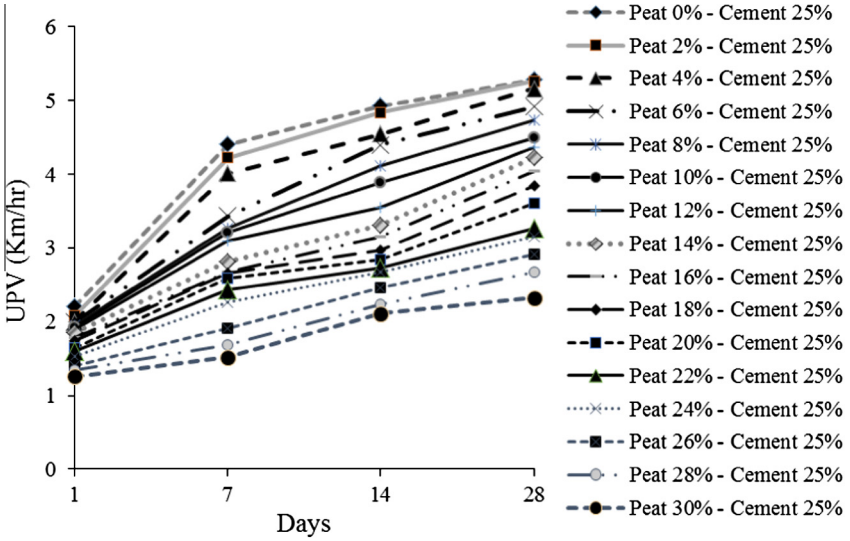

Fig. 8. Effect of peat inclusion (%) on the UPV (km/h) with the cement content of 25%.

peat content. For example, for samples with peat content increased from 0% to a value between 16% and 30%, the UPV value decreases from 5.29 km/h to a value between 4.05 and 2.33 km/h. On the other hand, among all the prepared samples, the sample with 30% cement and 0% peat showed the maximum UPV of 6.05 km/h after 28 days of curing. The minimum UPV of 1.14 km/h was observed on the 1st day of curing for the sample with 30% peat and 20% cement contents.

Another study reported that UPV values of peat-added brick decreased from 4 km/h to 0.56 km/h, without and with 54% peat in the brick mixture [33]. Singh and Siddique [42] successfully utilized UPV to test compressive strength of cement mixtures that were prepared by partial replacement of fine aggregates with the waste foundry sand. Since the waste foundry sand (WFS) gives better compaction than the peat, they observed initial increase in the UPV value for 15% WFS. However, for the WFS more than 15% in the cement mixture, sudden drop was seen in the UPV value.

The results of this study were compared to other similar studies that used UPV to determine strength of a mixture. Increased peat content was shown to decrease the UPV value. In addition, this study found that the UPV value increased as the curing period rose.

4.1.2. Cement's effect on UPV

The effect of cement content on the UPV is shown in Fig. 9. The graph shows UPV values for the samples with 20%, 25%, and 30% cement content and constant 20% peat content. As can be seen, the UPV increased as the cement content rose. The graph shows that for the sample with increased cement content from 20% to 25% and 30%, the UPV value increases from 3.25 km/h to a value between 3.61 and 4.04 km/h. Further, the graph shows that the curing period increases the UPV value. For example, the sample with 25% cement shows increased UPV value of 1.64 km/h, 2.59 km/h, 2.85 km/h, and 3.61 km/h for the 1st, 7th, 14th and 28th day of curing period, respectively.

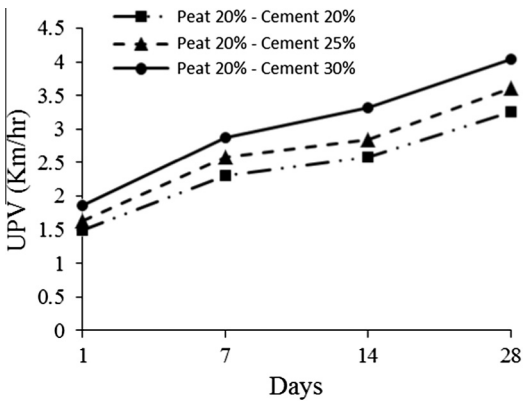

Fig. 9. Effect of the cement inclusion (%) on the UPV (km/h) with the peat content of 20%.

In a similar work [1], porosity of cementitious material was studied for partial saturation and dry condition using the UPV. As a result, increase of porosity from 8% to 13% deceased the UPV value from 4.8 km/h to 4.2 km/h. Our results are comparable with those results, where the pulse velocity decreased with increasing cement content based on the proportion of porosity and permeability. Furthermore, it is confirmed that increased cement content can result in increased UPV value. In addition, the UPV value increased as the curing period rose.

4.1.3. Effect of peat content on UCS

In this study, samples with 20%, 25% and 30% cement contents were prepared. The graph shows the UCS value for the sample with 25% cement, and increasing peat content from 0% to 30% in the interval of 2. Since there were 16 combinations of samples, the results are presented in two graphs (Figs. 10 and 11). Fig. 11 shows the UCS value for samples with the peat content ranging from 0% to 14%. Fig. 10 shows the UCS value for samples with the peat content ranging from 16% to 30%.

Fig. 10 shows that the UCS value decreases with increasing peat content. For example, the UCS value decreases from 36.92 MPa through 5.8 MPa to 3.37 MPa for the sample with 25% cement content as the peat content increases from 0% through 14% to 30%. Generally, longer curing period improves the UCS, regardless of the peat content (Figs. 10 and 11). For example, after 28 days of curing, the UCS value increases from 0.49 MPa to 3.38 MPa for the sample with 30% peat content. Also, for the overall sample, the maximum UCS value of 36.92 MPa was found for the specimen with 30% cement and 0% peat content. The minimum UCS value of 0.43 MPa was found in the specimen with 0% cement and 30% peat content.

This study observed decrease in the UCS value when the peat content increased. Nevertheless, the UCS increased for all the samples with aging, as shown in Figs. 10 and 11. We could not find any previous work that reported the UCS value for varying peat

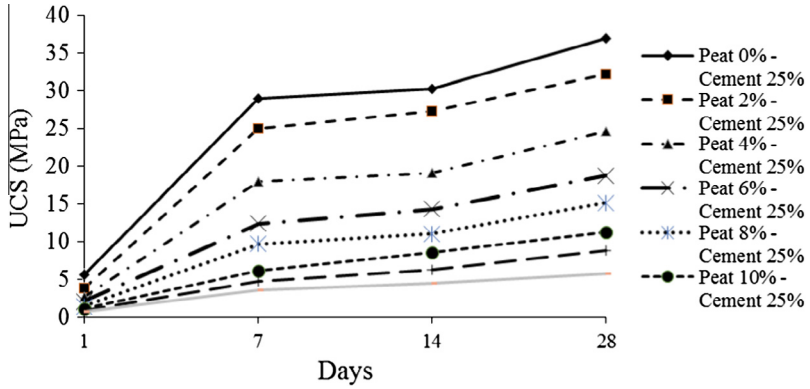

Fig. 10. Effect of the peat inclusion (0–14%) on the UCS with the cement content of 25%.

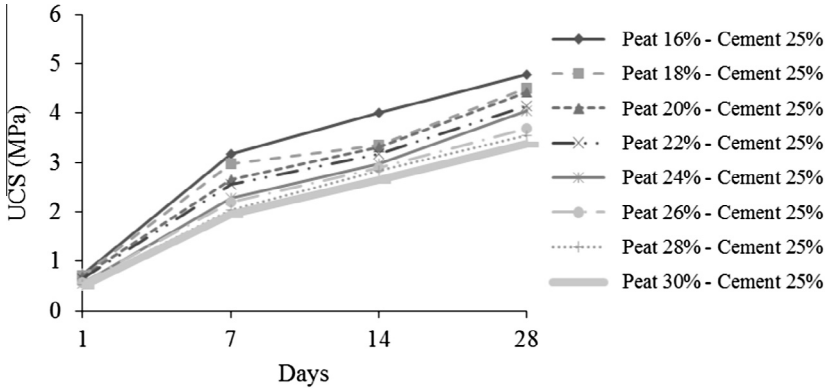

Fig. 11. Effect of the peat inclusion (16–30%) on the UCS with the cement content of 25%.

content. Only one study [43] evaluated the peat soil stabilization by adding the ground granulated blast furnace slag (GGBS) and MgO. Their UCS test results showed that for 5–20% of GGBS mix, the UCS increased with increased curing period. This supports the findings of our study that addition of peat decreases the UCS, while the UCS increases with increased curing time.

4.1.4. Cement's effect on UCS

Effect of cement content on the value of UCS in the samples is shown in Fig. 12. UCS of the samples increased once the cement content increased. The increasing value of UCS for the three compositions of cement was 20%, 25% and 30%, respectively. The graph shows that the value of UCS increases with increased curing period. For example, the sample containing 30% cement and 20% peat showed increase in the UCS through 0.77, 3.23, 3.73 and 4.7 MPa for the curing period of 1, 7, 14 and 28 days, respectively. Furthermore, among all the prepared samples, the sample with 20% cement and 20% peat showed the minimum UCS of 0.58 MPa on the 1st day of curing. The maximum UCS of 39.7 MPa was observed on the 28th day for zero peat content and 30% cement content.

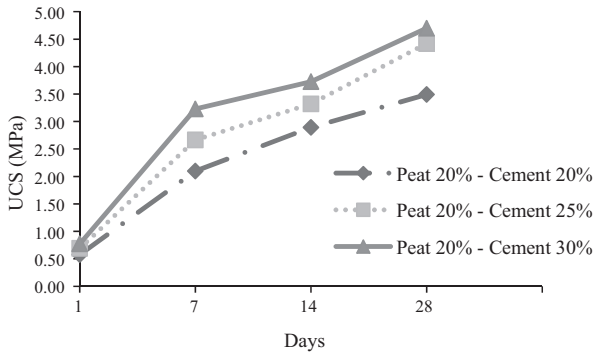

Fig. 12. Effect of the cement addition (%) on the UCS (MPa) with the peat content of 20%.

Kaniraj and Havanagi [44] reported that increased cement content in the fly ash soil mixture raised the strength and UCS. The current study also shows that for the peat-brick mixture, UCS value increases with raised cement content. Therefore, it can be established that the UCS value rises as the cement content and curing period increase.

4.1.5. Moisture's effect on UCS

Three classes of samples were made to inspect the UCS changes due to the moisture after 28 days of curing. The results are presented for the specimens with 15% moisture content, with the optimum moisture content (OMC), and with 5% moisture content. The moisture contents of 5% and 15% were adopted to avoid highly solid or soft textures (Figs. 13 and 14).

Fig. 13 shows the UCS for different cement content with 20% peat after 28 days of curing period. With 12.90% moisture content, the specimen with 20% peat and 30% cement had a UCS of 4.47 MPa. The UCS decreased to 1.96 MPa with the same composition when the MC was 15%. Similarly, the sample with the same mixture composition and 5% MC had a reduced UCS of 3.98 MPa. A sample of 25% cement and 20% peat under the OMC conditions showed 4.42 MPa of UCS, which was higher than the values logged with 15% and 5% MC. Therefore, it can be stated that the OMC conditions increases the UCS with a varied cement content and fixed

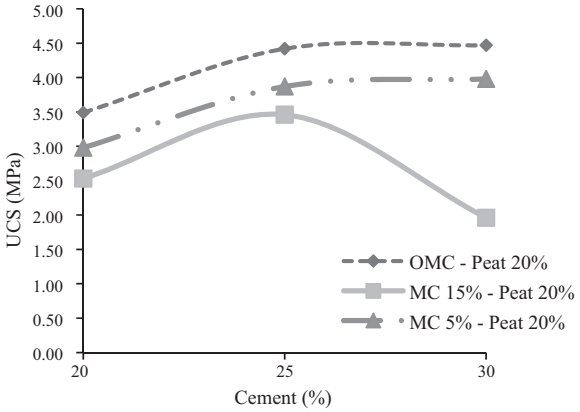

Fig. 13. The UCS (MPa) changes based on the moisture content with 20% peat and different cement inclusion after 28 days.

peat content. Consequently, lower MC is more satisfactory than a higher MC.

Fig. 14 shows variation of the samples' UCS with 25% cement and different peat values after 28 days of curing. The specimen with 25% cement and 10% peat had a UCS of 11.33 MPa under the moisture content of 12.90%. The UCS dropped to 2.86 MPa with 15% MC. Thus, the OMC should be maintained to ensure the integrity of peat–cement–sand mixture with a high UCS. The results of our study is in line with the previous works by Motamedi et al. [45,46], where similar trend was reported for the relationship between UCS and MC in mixtures of PFA–cement–sand.

4.2. ANFIS results

Table 6 presents statistical parameters of the calculated dataset. After selecting the most influential parameters, we analyzed the ANFIS model for the UPV estimation based on four inputs (Table 7). The ANFIS produced the RMS error of 0.026052 after the training. Fig. 15 shows the ANFIS decision surface for the UPV estimation of the four parameters.

The input (cement contents, peat, and sand of the sample for different curing periods) and output (ultrasonic pulse velocity) parameters were collected and defined for the learning techniques. Half of the data were used for training samples and the remaining 50% served for the testing samples.

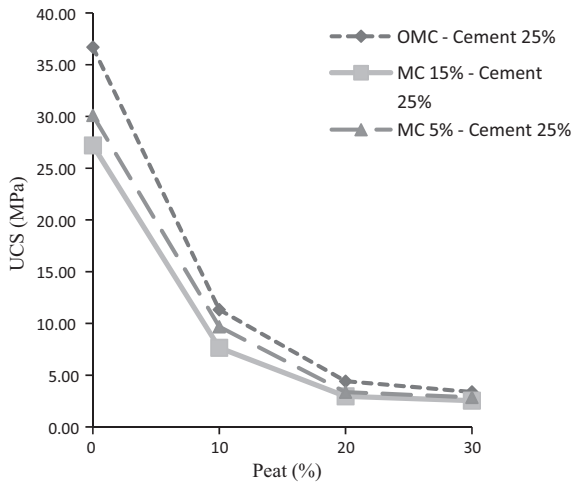

Fig. 14. The UCS (MPa) changes based on the moisture content with 25% cement content and different peat inclusions after 28 days.

Table 6
Statistical analysis for the input and output variables from the UPV experiment.

	Variable	Statistical parameters			
		Min	Max	Mean	Standard deviation
Outputs	UPV	1.14	6.05	3.06	1.18
Inputs	Peat (%)	0	30	15	9.52
	Cement (%)	20	30	25	24.90
	Sand (%)	40	80	60	10.19
	Curing period (days)	1	28	14	10.14

Table 7
Inputs and output for the sensitivity analysis of the ultrasonic pulse velocity.

	Physical property name
Input 1	Cement (%)
Input 2	Peat (%)
Input 3	Sand (%)
Input 4	Curing period

This section reports performance results of the ANFIS–UPV predictive models. Fig. 16 presents accuracy of the developed ANFIS–UPV predictive model using the testing dataset. It can be seen that most of the points fall within the diagonal line at the prediction model. Consequently, it follows that the prediction results are consistent with the values obtained from the ANFIS. This observation is confirmed with very high value for coefficient of determination. The training error is not a credible indicator for prediction potential of particular model; thus, we present the testing errors.

From the coefficient of determination ($R^2 = 0.9995$), it can be concluded that the anticipated values are rather similar to the observed values. The tests resulted in limited number of overestimated or underestimated values. Consequently, it is obvious that the predicted values have high level of precision.

4.2.1. Sensitivity analysis and discussion

The ANFIS process for variable selection (sensitivity analysis) was implemented in order to detect the predominant variables affecting the UPV prediction for the peat-enhanced bricks. Several methods were used to discover a subclass of the total logged parameters, showing noble capability of prediction. The ANFIS network was used to perform a variable search and to determine the way that input parameters influence UPV prediction for the peat-enhanced bricks (Table 7).

A comprehensive search was performed in order to choose the set of ultimate optimal combination inputs (cement, peat, sand contents and curing period) with the highest impact on the output parameter. Basically, an ANFIS model was built by functions for each combination, which were then trained for the single epoch. From the outset, the most impactful input in the prediction of the output was identified and determined, as depicted in Fig. 17. The input variables on the left-hand side have the lowest number of errors or the most relevance with regards to the outcome (Fig. 17).

As it can be clearly seen, the input variable 4 (the curing period) is the most influential for the UPV prediction of the peat-enhanced bricks. The fact that both checking errors and training are comparable is an indirect indication that there is no over fitting. This means that selection of more than one input parameter in the construction of the ANFIS model can be explored. For the verification purposes, the best integration of two receiving parameters was explored. The results listed in Table 8 show the optimal combinations of two input attributes for the prediction of the UPV of the peat-enhanced bricks. The results indicated that among all the examined parameters, optimal combination of peat content and

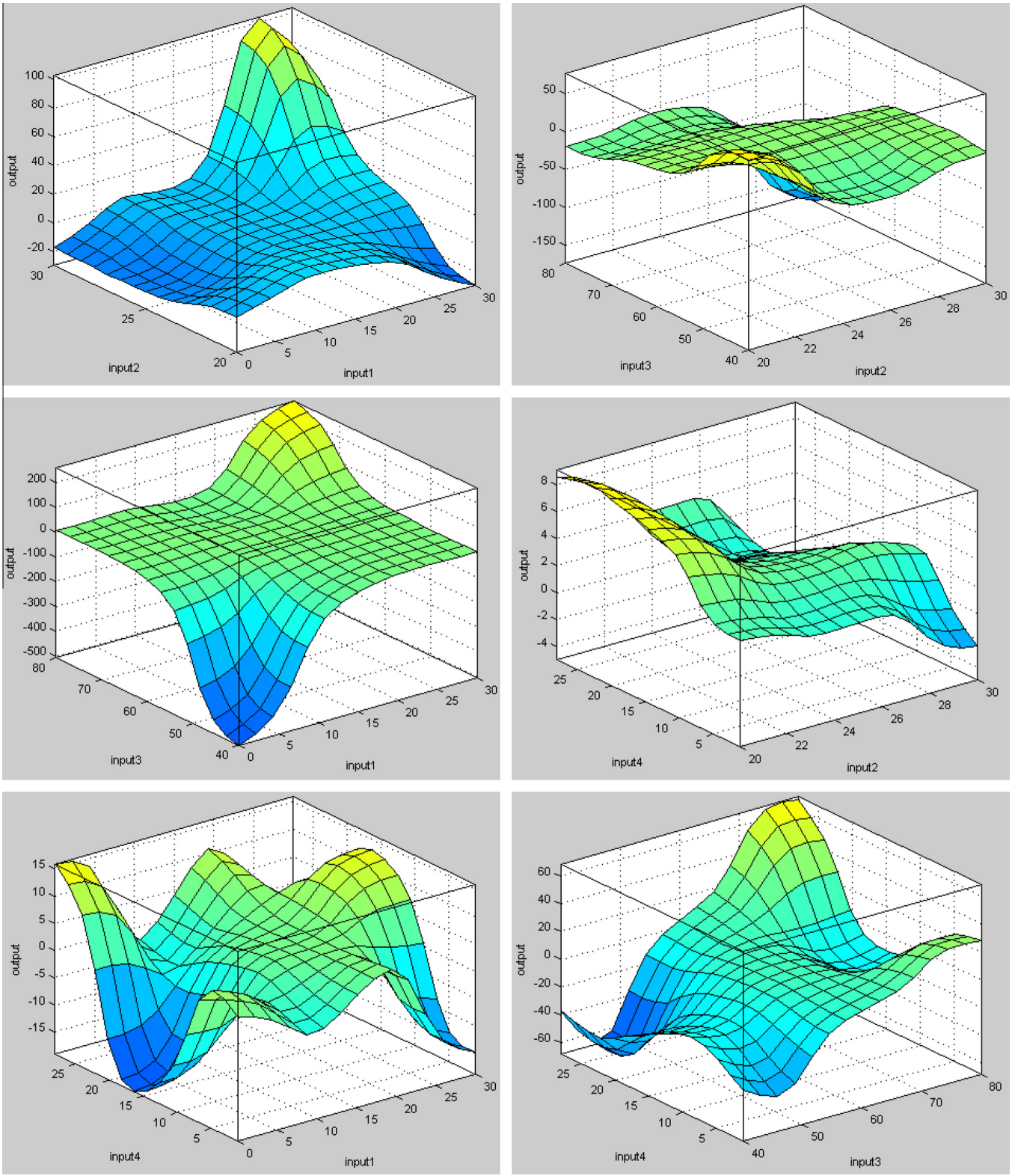

Fig. 15. The ANFIS decision surface for the UPV estimation; input1: peat, input2: cement, input3: sand, and input4: curing period.

curing period is the most influential on the UPV and the best predictor of accuracy. A model with such structural simplicity is always preferred; the use of more than two inputs in the construction of ANFIS model may not be appropriate. Therefore, the two-input ANFIS should be the basis for further examination. Then, the input parameters that were chosen from the initial training and checking datasets were extracted.

To enable the ANFIS and find the right inputs quickly, the function only trained each variable at a time. Once the inputs were fixed, the 100 epochs on the ANFIS training were increased. The

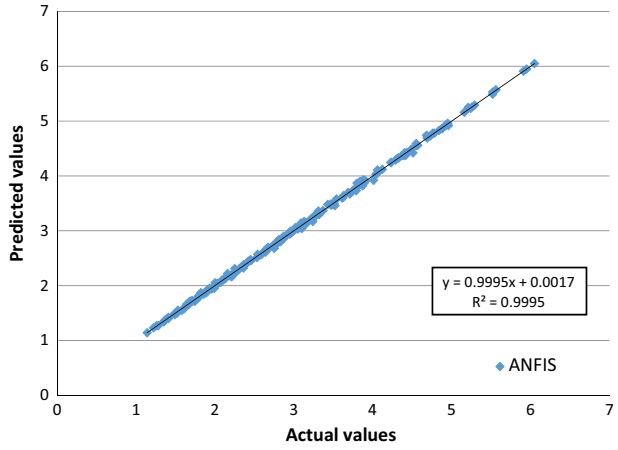

Fig. 16. Performance of the ANFIS for ultrasonic pulse velocity estimation.

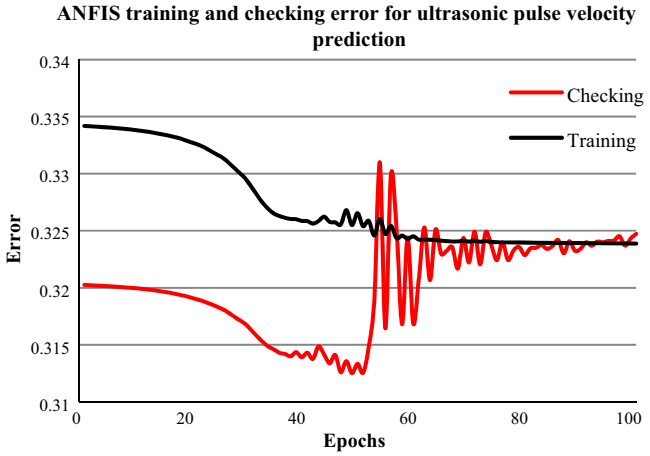

Fig. 18. The ANFIS checking and training errors for the two selected inputs for the UPV prediction of the peat-enhanced bricks.

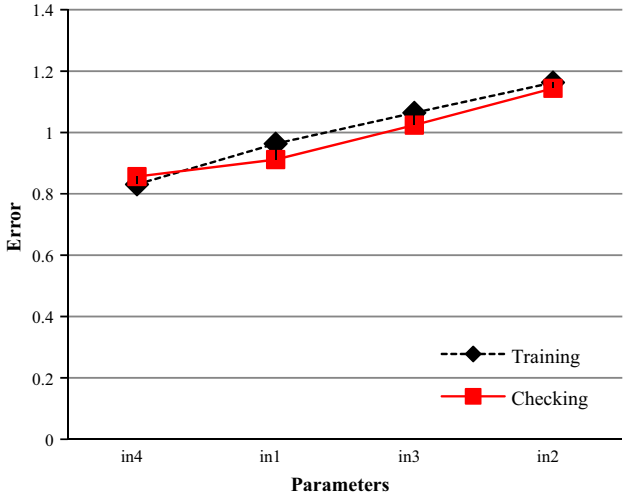

Fig. 17. Influence of every input parameter on the UPV of the peat-enhanced bricks.

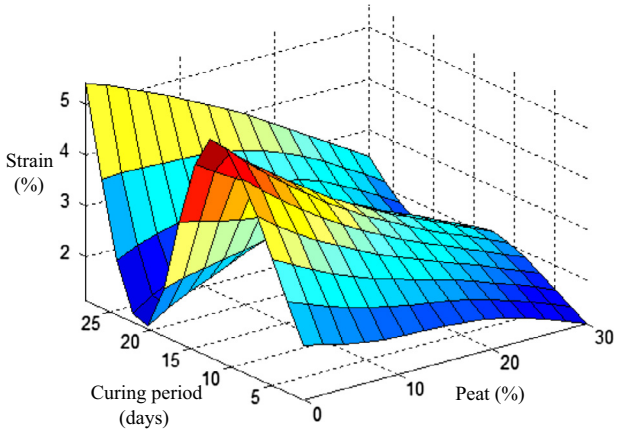

Fig. 19. The ANFIS expected correlation between the most effective parameters and UPV of the peat-enhanced bricks.

Table 8
The ANFIS regression errors for the UPV prediction of the peat-enhanced bricks.

	Peat (%)	Cement (%)	Sand (%)	Curing period (day)
Peat (%)	trn = 0.9635, chk = 0.9118	trn = 0.9152, chk = 0.8657	trn = 0.9145, chk = 0.8662	trn = 0.3342, chk = 0.3203
Cement (%)		trn = 1.1630, chk = 1.1440	trn = 0.9153, chk = 0.8659	trn = 0.7734, chk = 0.8067
Sand (%)			trn = 1.0642, chk = 1.0242	trn = 0.5794, chk = 0.5845
Curing period (day)				trn = 0.8310, chk = 0.8564

error curves for these 100 epochs for the two extracted input parameters are shown in Fig. 18. The training errors and the checking errors are represented by the dashed curve and solid curve, respectively.

The ANFIS predictions were compared by a linear regression model through equating individual RMS values against the checking data. The linear regression error was 0.423 and the regression error was 0.313. It is clear that the ANFIS model performs better than the linear regression model. Fig. 19 shows the graph of the ANFIS model of input–output surface (decision) for prediction of the UPV of the peat-enhanced bricks as monotonic non-linear surface. It also illustrates the response of ANFIS model for varying selected input parameters.

5. Conclusions

This paper described a method for the estimation of ultrasonic pulse velocity using the ANFIS soft computing methodology. Based on the results, the ANFIS method can estimate the distribution of ultrasonic pulse velocity with high accuracy. Also, it can be concluded that the UPV is affected by the properties of materials. This study considered various combinations of peat–cement–sand mixtures to conduct the UPV test. The peat-enhanced brick specimens were cuboidal in shape. It can be stated that increased peat content in the peat–cement–sand specimen decreases the UPV value, whereas increased curing period raises the UPV value. Furthermore, increased cement content raises the UPV value.

Based on the variable selection analysis, it is apparent that the cement has the highest sensitivity on the UPV, while peat has the smallest sensitivity on output. It might be concluded that ANFIS is an efficient tool for predicting UPV in accordance with the percentage content of the input variable.

In addition, the brick moisture affects the UPV. Water in pore material structure (replacing the displaced air) increases the UPV. This study attempted to determine unambiguous moisture

conditions during the testing to ensure repeatability and reproducibility of the measurement.

Acknowledgements

We sincerely thank the editor and the reviewers for their constructive comments. The authors express their sincere thanks for the funding support they received from the HIR-MOHE University of Malaya under Grants Nos. UM.C/HIR/MOHE/ENG/34, and M.C/HIR/MOHE/ENG/47. This research was supported by Basic Science Research Program through the National Research Foundation of Korea (NRF) funded by the Ministry of Science, ICT & Future Planning (No. NRF-2013R1A1A1060052).

References

[1] Z. Lafhaj, M. Goueygou, A. Djerbi, M. Kaczmarek, Correlation between porosity, permeability and ultrasonic parameters of mortar with variable water/cement ratio and water content, Cem. Concr. Res. 36 (4) (2006) 625–633.
[2] Y.S. Cho, Non-destructive testing of high strength concrete using spectral analysis of surface waves, NDT & E Int. 36 (4) (2003) 229–235.
[3] R. Solis-Carcaño, E.I. Moreno, Evaluation of concrete made with crushed limestone aggregate based on ultrasonic pulse velocity, Constr. Build. Mater. 22 (6) (2008) 1225–1231.
[4] Y. Yang, M.D. Lepech, E.-H. Yang, V.C. Li, Autogenous healing of engineered cementitious composites under wet–dry cycles, Cem. Concr. Res. 39 (5) (2009) 382–390.
[5] T. Ozturk, O. Kroggel, P. Grubl, J.S. Popovics, Improved ultrasonic wave reflection technique to monitor the setting of cement-based materials, NDT and E Int. 39 (4) (2006) 258–263.
[6] S. Granger, A. Loukili, G. Pijaudier-Cabot, G. Chanvillard, Experimental characterization of the self-healing of cracks in an ultra high performance cementitious material: Mechanical tests and acoustic emission analysis, Cem. Concr. Res. 37 (4) (2007) 519–527.
[7] S.M. Islam, R. Hashim, A. Saiful Islam, Behaviour of peat-added composite bricks in low-cost building construction, Mater. Res. Innovations 18 (S6) (2014). S6-1–S6-5.
[8] Leong Sing Wong, Roslan Hashim, Faisal Ali, Improved strength and reduced permeability of stabilized peat: Focus on application of kaolin as a pozzolanic additive, Constr. Build. Mater. 40 (2013) 783–792. ISSN: 0950-0618.
[9] M. Ohtsu, The history and development of acoustic emission in concrete engineering, Mag. Concr. Res. 48 (177) (1996) 321–330.
[10] H.Y. Qasrawi, Concrete strength by combined nondestructive methods – simply and reliably predicted, Cem. Concr. Res. 30 (5) (2000) 739–746.
[11] B. Hobbs, M.T. Kebir, Non-destructive testing techniques for the forensic engineering investigation of reinforced concrete buildings, Forensic Sci. Int. 167 (2–3) (2007) 167–172.
[12] M. Bilgehan, P. Turgut, Artificial neural network approach to predict compressive strength of concrete through ultrasonic pulse velocity, Res. Nondestr. Eval. 21 (1) (2010) 1–17.
[13] J.H. Bungey, M.N. Soutsos, Reliability of partially-destructive tests to assess the strength of concrete on site, Constr. Build. Mater. 15 (2–3) (2001) 81–92.
[14] P.R. Rajagopalan, J. Prakash, V. Naramimhan, Correlation between ultrasonic pulse velocity and strength of concrete, Indian Concr. J. 47 (11) (1973) 416–418.
[15] Y. Lin, C.-P. Lai, T. Yen, Prediction of ultrasonic pulse velocity (UPV) in concrete, ACI Mater. J. 100 (1) (2003) 21–28.
[16] S.K. Sahu, K.K. Jain, Assessment of concrete quality from pulse velocity tests, non-destructive testing, Civil Eng. Rev. (1998) 43–45.
[17] A. Ikpong, The relationship between the strength and non-destructive parameters of rice husk ash concrete, Cem. Concr. Res. 23 (2) (1993) 387–398.
[18] G. Ye, P. Lura, K. Van Breugel, A. Fraaij, Study on the development of the microstructure in cement-based materials by means of numerical simulation and ultrasonic pulse velocity measurement, Cement Concr. Compos. 26 (5) (2004) 491–497.
[19] ASTM C597-83, Standard Test Method for Pulse Velocity Through Concrete, ASTM International, West Conshohocken, PA, 1991.
[20] P.K. Mehta, P.J. Monteiro, Concrete: microstructure, properties, and materials, vol. 3.
[21] M. Sharma, B. Gupta, Sonic modulus as related to strength and static modulus of high strength concrete, Indian Concr. J. 34 (4) (1960) 139–141.
[22] E.A. Whitehurst, Soniscope tests concrete structures, in: ACI Journal Proceedings, ACI, 1951.
[23] K. Tharmaratnam, B. Tan, Attenuation of ultrasonic pulse in cement mortar, Cem. Concr. Res. 20 (3) (1990) 335–345.
[24] P. I. IS 13311, Standard Code of Practice for Non-Destructive Testing of Concrete: Part 1—Ultrasonic Pulse Velocity, Bureau of Indian Standards, New Delhi, 1992.
[25] E. Marfisi, C. Burgoyne, M. Amin, L. Hall, The use of MRI to observe the structure of concrete, Mag. Concr. Res. 57 (2) (2005) 101–109.
[26] I. Prassianakis, P. Giokas, Mechanical properties of old concrete using destructive and ultrasonic non-destructive testing methods, Mag. Concr. Res. 55 (2) (2003) 171–176.
[27] C. Vipulanandan, V. Garas, Electrical resistivity, pulse velocity, and compressive properties of carbon fiber-reinforced cement mortar, J. Mater. Civ. Eng. 20 (2) (2008) 93–101.
[28] H. Yıldırım, O. Sengul, Modulus of elasticity of substandard and normal concretes, Constr. Build. Mater. 25 (4) (2011) 1645–1652.
[29] G. Trtnik, F. Kavcic, G. Turk, Prediction of concrete strength using ultrasonic pulse velocity and artificial neural networks, Ultrasonics 49 (1) (2009) 53–60.
[30] G. Trtnik, G. Turk, Influence of superplasticizers on the evolution of ultrasonic P-wave velocity through cement pastes at early age, Cem. Concr. Res. 51 (2013) 22–31.
[31] Ç., U.Z., K., T., M., K. Effect of mineral admixtures on the correlation between ultrasonic velocity and compressive strength for self-compacting concrete. Russ. J. Nondestruct. Test. 44(5) (2008) 367–374.
[32] B.S. Mohammed, N.J. Azmi, M. Abdullahi, Evaluation of rubbercrete based on ultrasonic pulse velocity and rebound hammer tests, Constr. Build. Mater. 25 (3) (2011) 1388–1397.
[33] S.M. Islam, R. Hashim, A. Islam, R. Kurnia, Effect of peat on physicomechanical properties of cemented brick, Sci. World J. 2014 (2014).
[34] S. Deboucha, R. Hashim, A. Alwi, Engineering properties of stabilized tropical peat soils, Electron. J. Geotech. Eng. 13 (2008) 1–9.
[35] ASTM International, ASTM D5239-12, Standard Practice for Characterizing Fly Ash for Use in Soil Stabilization, West Conshohocken, PA, 2012.
[36] G.W. Clough, J. Iwabuchi, N.S. Rad, T. Kuppusamy, Influence of cementation on liquefaction of sands, J. Geotech. Eng. 115 (8) (1989) 1102–1117.
[37] S. Kolias, V. Kasselouri-Rigopoulou, A. Karahalios, Stabilisation of clayey soils with high calcium fly ash and cement, Cement Concr. Compos. 27 (2) (2005) 301–313.
[38] J. Stevens, Unified soil classification system, Civil Eng.—ASCE 52 (12) (1982) 61–62.
[39] Radu-Emil Precup, Hans Hellendoorn, A survey on industrial applications of fuzzy control, Comput. Ind. 62 (3) (2011) 213–226.
[40] T. Takagi, Derivation of fuzzy control rules from human operator's control actions, in: Proceedings of the IFAC Symposium on fuzzy Information, Knowledge Representation and Decision Analysis, SMC-15(1), 1983, pp. 55–60.
[41] T. Takagi, M. Sugeno, Fuzzy identification of systems and its applications to modeling and control, Syst., Man Cybern., IEEE Trans. 1 (1985) 116–132.
[42] G. Singh, R. Siddique, Effect of waste foundry sand (WFS) as partial replacement of sand on the strength, ultrasonic pulse velocity and permeability of concrete, Constr. Build. Mater. 26 (1) (2012) 416–422.
[43] Y. Yi, M. Liska, A. Al-Tabbaa, Properties of two model soils stabilized with different blends and contents of GGBS, MgO, Lime, and PC, J. Mater. Civ. Eng. 26 (2) (2013) 267–274.
[44] S.R. Kaniraj, V.G. Havanagi, Compressive strength of cement stabilized fly ash-soil mixtures, Cem. Concr. Res. 29 (5) (1999) 673–677.
[45] Shervin Motamedi, Ki.-Il Song, Roslan. Hashim, Prediction of unconfined compressive strength of pulverized fuel ash–cement–sand mixture, Mater. Struct. 48 (4) (2015) 1061–1073.
[46] S. Motamedi, et al., Application of adaptive neuro-fuzzy technique to predict the unconfined compressive strength of PVA–sand–cement mixture, Powder Technol. (2015), http://dx.doi.org/10.1016/j.powtec.2015.02.045.
[47] Shervin Motamedi, Shahaboddin Shamshirband, Dalibor Petković, Roslan Hashim, Application of adaptive neuro-fuzzy technique to predict the unconfined compressive strength of PFA-sand-cement mixture, Powder Technol. 278 (2015) 278–285.
[48] Shahaboddin Shamshirband, Dalibor Petković, Roslan Hashim, Shervin Motamedi, Nor Badrul Anuar, An appraisal of wind turbine wake models by adaptive neuro-fuzzy methodology, Int. J. Elec. Power. 63 (2015) 618–624.
[49] Shahaboddin Shamshirband, Dalibor Petković, Roslan Hashim, Shervin Motamedi, Adaptive neuro-fuzzy methodology for noise assessment of wind turbine, PloS one 9 (7) (2014) e103414.